Transaction B: Mechanical Engineering
Vol. 17, No. 4, pp. 301–314

SCIENTIA IRANICA

Comparison of the Mollification Method, Wavelet Transform and Moving Average Filter for Reduction of Measurement Noise Effects in Inverse Heat Conduction Problems

S.D. Farahani[1,*] and F. Kowsary[1]

Abstract. *This paper proposes a procedure to smooth temperature data by wavelet transform, moving average filter and the mollification method prior to utilizing the IHCP methods (i.e. the conjugate gradient method, the Tikhonov regularization method) for unknown heat flux estimation. The measured transient temperature data utilized in the solution may be obtained from locations inside the body or from locations on its inactive boundaries. Two case studies are used to investigate the efficiency and accuracy of the mentioned procedure. The first case study is performed on a rectangular body. The second case study demonstrates the ability of the proposed method to estimate heat flux in a more complicated geometry. Smoothing measured data causes an increase in the accuracy and stability of the estimation.*

Keywords: *Mollification method; Wavelet transform; Moving average filter; Estimated heat flux; Conjugate gradient method; Tikhonov regularization method.*

INTRODUCTION

Inverse Heat Conduction Problems (IHCP) have recently found wide applications in industry. The classical heat conduction problem, where the temperature histories at the surface of the body are a known function time and interior temperature distribution is then determined, is termed a direct problem. Inverse Heat Conduction Problems (IHCP) involve estimation of surface boundary conditions (i.e. heat flux or temperature [1-3]), thermophysical properties [4-5], an unknown geometry of a section of a body [6], or volumetric heat generation [7] using some temperature measured from locations within or on the surface of the body. IHCPs are mathematically ill-posed being highly sensitive to random errors (noise) that inherently exist in measured temperature data. In order to alleviate this problem, regularization techniques are utilized [8]. In general, methods of solving inverse heat conduction problems can be divided into two main groups: sequential methods and whole domain methods. Each of the groups has its own advantages. Sequential methods can be used for real time estimation and require less memory and computational time. Whole domain methods on the other hand are more accurate as compared to sequential methods, since whole domain methods use all the measured temperature simultaneously in estimation of any unknown parameters or functions. Well-known whole domain methods are the conjugate gradient method and the Tikhonov regularization method. The conjugate gradient method has been used widely in the literature and known as one of the successful algorithms of IHCP especially for problems whose boundary conditions cover a major part of the boundary [9].

An analytical solution was presented by Imber for a solid cylinder with radial and angular heat flux dependence [10]. Kakaee et al. used the Levenberg, Marquardt and Modified Levenberg methods to estimate the surface temperature on a moving boundary in the burning process of a homogenous solid fuel [11]. Heydari et al. studied gas temperature estimation in a partially filled rotating cylinder by using the conjugate gradient method and Levenberg-Marquardt method [12]. Kowsary et al. suggested a Variable Metric Method (VMM) for solving inverse heat con-

1. *Department of Mechanical Engineering, University of Tehran, Tehran, P.O. Box 14395-515, Iran.*
*. *Corresponding author. E-mail: sdavoodabadifarahani@gmail.com*

Received 17 September 2009; received in revised form 15 March 2010; accepted 21 June 2010

duction problems [13]. In another work, Kowsary et al. suggested a transformation matrix based on the dual reciprocity boundary element along with the sequential function specification scheme for solving two-dimensional inverse heat conduction problems involving unknown time and space varying boundary heat flux estimation [14]. Some researchers have attempted to filter measured temperature data from the sensors before employing the IHCP algorithm; for example, Al-Khalidy used digital filter formulation to smooth noisy sensor data in parabolic and hyperbolic inverse heat conduction [15]. Ji and Jang used a Kalman filter to filter noisy sensor data and solve one dimensional IHCP [16]. Beck et al. proposed a prefiltering formula in which all data is replaced by $y_m = (y_{m-1} + 2y_m + y_{m+1})/4$, when m is the time index [1]. Kowsary et al. utilized wavelets to reduce the destructive nature of existing noise contaminating temperature data in inverse heat conduction problems [17].

In this paper, the mollification method, Wavelet transform and moving average filter are used to smooth experimental data prior to the use of IHCP algorithms. Whole domain methods, such as the Tikhonov regularization method and the conjugate gradient method, are used to estimate unknown temporally and spatially varying boundary heat flux. The mathematical concept of formal stability for the mollification method was originally introduced by Manselli and Miller [18] and then extended by Murio [19-21]. Noise reduction by wavelet as proposed by Donoho and Johnstone (1991) and Donoho (1993) and referred to as de-noising is distinctly different from other noise reduction approaches, such as the high-frequency filtering of signal components [22-24]. The moving average filter is the most common filter, mainly because it is the easiest digital filter to understand and use. In spite of its simplicity, the moving average filter is optimal for reducing random noise of a signal.

In this paper, the Finite Element method is used in numerical solutions where ANSYS capabilities are utilized in the mesh generation and numerical solution of the problem, in order to evade the need for coding the direct heat conduction problem. By simulating the problem in the graphic user interface of the software and saving it in the form of a function, the numerical solution of the problem can be performed merely by calling the saved function. Inverse algorithms are written in ANSYS Parametric Design Language (APDL).

THE MOLLIFICATION METHOD

The mollification method is a regularization method that uses the averaging property of the Gaussian kernel to smooth noisy data. In this work, the method presented by Murio is used [20]. The automatic character of the mollification algorithm, which makes it highly competitive, is due to incorporation of the Generalized Cross Validation (GCV) procedure for the selection of the radius of mollification as a function of the perturbation level in the data, which is generally unknown. In this section, we introduce the method.

Abstract Setting

Let $\rho > 0$, $\delta > 0$ and $A_\rho = (\int_{-\rho}^{\rho} \exp(-s^2)ds)^{-1}$. The δ-mollification of an integrable function is based on convolution with the kernel:

$$\rho_{\delta,\rho}(t) = \begin{cases} A_\rho \delta^{-1} \exp(-t^2/\delta^2) & |t| < \rho\delta \\ 0 & |t| > \rho\delta \end{cases} \tag{1}$$

The δ-mollifier ρ_δ function is a nonnegative $C^\infty(-\rho\delta, \rho\delta)$, vanishing outside $(-\rho\delta, \rho\delta)$ and satisfying:

$$\int_{-\rho\delta}^{\rho\delta} \rho_{\delta,\rho}(t)dt = 1. \tag{2}$$

Let $I = [0,\ 1]$ and $I_\delta = [-\rho\delta, \rho\delta]$. The interval I is nonempty whenever $\rho\delta < 1/2$.

If f is integrable on I, we define its δ-mollification on I by the convolution integral:

$$J_\delta f(t) = \int_0^1 \rho_\delta(t-s)f(s)ds. \tag{3}$$

Discrete Mollification

In order to define the δ-mollification of a discrete function, we consider n different numbers on I, say $t_1, t_2, \cdots, t_n$ satisfying and defining:

$$\Delta t = \max_{1 \le j \le n-1} |t_{j+1} - t_j|,$$

$$0 \le t_1 \le \cdots \le t_n \le 1.$$

Furthermore, we set $s_0 = 0$, $s_n = 1$ and for $j = 1, 2, \cdots, n-1$, $s_j = \frac{1}{2}(t_j + t_{j-1})$.

Let $G = \{g_j\}_{j=1}^n$ be a discrete function defined on the set $k = \{t_1, t_2, \cdots, t_n\}$.

The discrete δ-mollification of G is defined as follows. For every $t \in I_\delta$:

$$g_s(t) = \sum_{j=1}^{n} \left(\int_{s_{j-1}}^{s_j} \rho_\delta(t-s)ds \right) g_j. \tag{4}$$

Notice that:

$$\sum_{j=1}^{n}\left(\int_{s_{j-1}}^{s_j}(\rho_\delta(t-s)ds)\right)=\int_{-\rho\delta}^{\rho\delta}\rho_\delta(s)ds=1.$$

Selection of Regularization Parameters

Computation of $(g_\delta^\varepsilon)_k$ can be viewed as:

$$\sum_{i=1}^{n}[A_\delta]_{k_i}g_i^\varepsilon=(g_\delta^\varepsilon)_k, \tag{5}$$

where:

$$[A_\delta]_{k_i}=\int_{s_{j-1}}^{s_j}\rho_\delta(t_k-s)ds, \tag{6}$$

and $G=\{g_i^\varepsilon\}_{i=0}^N$ is the noisy data function. Since the noise in the data is unknown, an appropriate mollification parameter introducing the correct degree of smoothing should be selected. Such a parameter is determined by the principle of generalized cross validation as the value of δ that minimizes the functional:

$$\frac{(G^\varepsilon)^T(I^T-A_\delta^T)(I-A_\delta)G^\varepsilon}{\text{Trace }((I^T-A_\delta^T)(I-A_\delta))}. \tag{7}$$

After computing g_δ^ε, the desired δ-minimizer is obtained by a golden section search procedure.

Extension of Data

Computation of g_δ and $J_\delta g$ throughout the time domain $I=[0,\ 1]$ requires either the extension of g to a slightly bigger interval $[-\rho\delta, 1+\rho\delta]$ or consideration of g restricted to the subinterval $[\rho\delta, 1-\rho\delta]$. Our approach is the first one.

We search for constant extensions, g^* of g, to the intervals $[-\rho\delta, 0]$ and $[1, 1+\rho\delta]$ satisfying the conditions:

$$\|J_\delta(g^*)-g\|_{l^2(0,\rho\delta)}\ \text{ is minimum}, \tag{8}$$

and:

$$\|J_\delta(g^*)-g\|_{l^2(1-\rho\delta,0)}\ \text{ is minimum}. \tag{9}$$

The unique solution to this optimization problem at the boundary $x=1$ is given by:

$$g^*=\frac{\int_{1-\rho\delta}^{1}\left(g(t)-\int_0^1\rho_\delta(t-s)g(s)dt\right)\left(\int_1^{1+\rho\delta}\rho_\delta(t-s)ds\right)dt}{\int_{1-\rho\delta}^{1}(\int_1^{1+\rho\delta}\rho_\delta(t-s)ds)^2dt}. \tag{10}$$

A similar result holds at end point $x=0$.

WAVELET TRANSFORM

Wavelets are classes of function with properties that are considered highly suitable for analysis of a wide spectrum of signals found in engineering and scientific applications. Wavelets are used as basic functions for signal decomposition and reconstruction described briefly as follows.

For a scalar function, $\psi(t): R\to R$, to be treated as a wavelet, it is necessary that $\psi(t)$ satisfy the following conditions:

1. To have a finite norm, i.e.:

$$\int_{-\infty}^{\infty}|\psi(t)|^2\,dt<\infty.$$

2. To have a finite support width (actual or effective) both in the time and frequency domain (to be band limited).
3. To satisfy the admissibility condition defined as:

$$\int_{-\infty}^{\infty}\left|\frac{\hat\psi(w)}{w}\right|^2dw<\infty, \tag{11}$$

where $\hat\psi(w)$ is the Fourier transform of $\psi(w)$.

The admissibility condition refers to the $\hat\psi(w)$ behavior near the origin where it is required to approach zero faster than frequency variable w. The admissibility condition implies having a zero DC (average) value, i.e.:

$$\int_{-\infty}^{\infty}\psi(t)dt=0.$$

Wavelets assume different forms; they can be symmetric or asymmetric. The wavelet transform of function $f(t)$ is defined as:

$$W_{a,b}=\int_{-\infty}^{\infty}f(t)\psi\left(\frac{(t-b)}{a}\right)dt,\qquad a\neq 0, \tag{12}$$

where scalars a and b are referred to as scale and translation factors, respectively. Now, let scaling and translation parameters, a and b, assume the following discrete values:

$$\begin{cases}a=2^j\\ b=k2^{-j}\end{cases}\qquad j,k\in z. \tag{13}$$

Then, the translated and scaled version of $\Psi(t)$ can be written as:

$$\psi_{j,k}=2^{j/2}\psi(2^jt-k),\qquad j,k\in Z. \tag{14}$$

$\psi_{j,k}$ constitute a family of wavelet functions constructed from a prototype of wavelet function $\Psi(t)$.

They are utilized as basic functions for function (signal) expansion. Signal expansion using discrete values of a and b of Equation 12 is referred to as DWT.

Analysis of given data in wavelet transform consists of three main stages:

1. Decomposition,
2. Analysis,
3. Reconstruction.

Decomposition Stage

In the decomposition stage, as used in DWT, a given signal is decomposed into a set of low and high frequencies. Decomposition of a signal into a set of hierarchically low and high frequency components was proposed first by Mallt [24,25].

Analysis and Signal Manipulation Stage

This stage of the wavelet analysis of a signal includes the manipulation and coding of wavelet coefficients, such as for noise reduction, information extraction, data compression, and data transmission. Thresholding of wavelet coefficients is a commonly used form of manipulation of coefficients for noise reduction.

Synthesis Stage

Finally, the synthesis stage refers to signal reconstruction, where in reverse transformation is applied to manipulated (modified) coefficients. Manipulation of coefficients results in a set of modified values for coefficients used during the reconstruction (synthesis) stage of the signal.

Wavelet-Based Noise Reduction

Noise reduction by wavelets is based on the property of the wavelet transform referred to as the sparsity of signal representation in the coefficient domain. Sparsity refers to a clustering of coefficients into two groups of:

1. A few large amplitude coefficients.
2. A large number of small valued coefficients.

Small amplitude coefficients are attributed to the noise content of the signal. Noise reduction by wavelets deals with the manipulation of wavelet coefficients in which coefficients below a judiciously selected threshold level are replaced by zero, and the inverse transform of manipulated (modified) coefficients is used to recover denoised signals; hence, noise is cleaned from the signal. Two approaches can be considered for thresholding:

1. **Hard Thresholding**. In hard thresholding, only wavelet coefficients with absolute values below or at the threshold level are affected; they are replaced by zero while others are kept unchanged. Modification of coefficients ω in hard thresholding can be described as follows:

$$W_m = W \quad \text{if} \quad |W| \geq th,$$

$$W_m = 0 \quad \text{if} \quad |W| < th. \tag{15}$$

2. **Soft Thresholding**. In soft thresholding, coefficients above the threshold level are also modified where they are reduced by the amount of threshold:

$$W_m = \text{Sign}(W)(|W| - th) \quad \text{if} \quad |W| \geq th,$$

$$W_m = 0 \quad \text{if} \quad |W| < th. \tag{16}$$

MOVING AVERAGE FILTER

The moving average is the most common filter, mainly because it is the easiest digital filter to understand and use. In spite of its simplicity, the moving average filter is optimal for reducing the random noise of a signal. A moving average filter smoothes data by replacing each data point with the average of the neighboring data points defined within the span. This process is equivalent to low pass filtering with the response of the smoothing given by the difference equation:

$$y_s(i) = \frac{1}{2N+1}(y(i+N) + y(i+N-1) + \cdots + y(i-N)), \tag{17}$$

where $y_s(i)$ is the smoothed value for the ith data point, N is the number of neighboring data points on either side of $y_s(i)$, and $2N+1$ is the span. The moving average smoothing method used by curve fitting follows these rules:

1. The span must be odd.
2. The data point to be smoothed must be at the center of the span.
3. The span is adjusted for data points that cannot accommodate the specified number of neighbors on either side.
4. The end points are not smoothed because a span cannot be defined.

INVERSE PROBLEM STATEMENT

Inverse estimation of time varying heat flux is considered in two case studies. The first case study is performed on a rectangular body as shown in Figure 1. The geometry and boundary conditions of the first test case are presented, as well as the locations of the

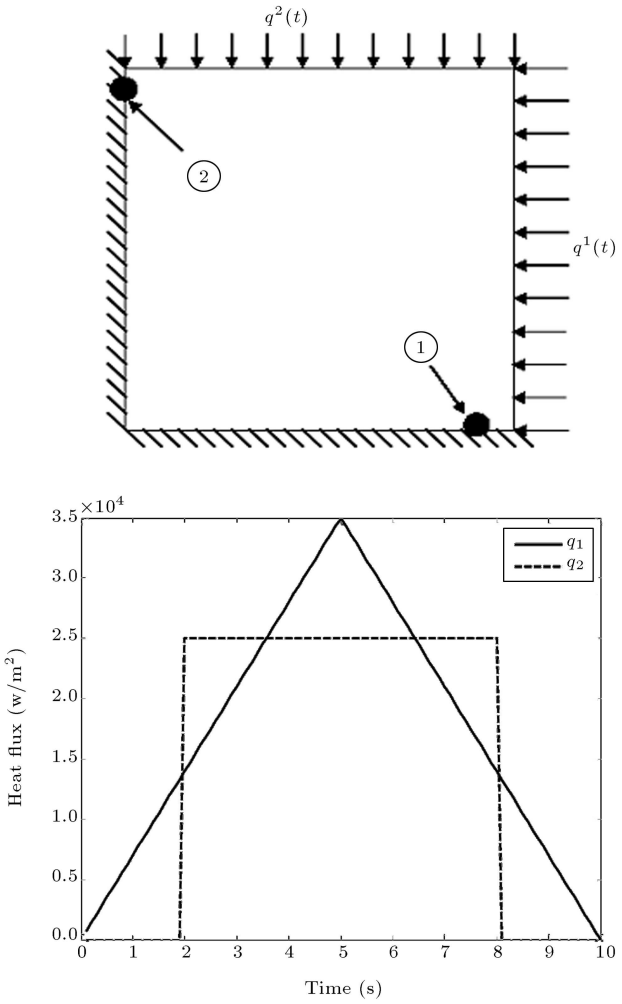

Figure 1. Geometry and boundary conditions of the first case study.

sensors. Assuming constant thermal properties, the heat equation is written as:

$$\frac{\partial^2 T}{\partial x^2} + \frac{\partial^2 T}{\partial y^2} = \frac{1}{\alpha}\frac{\partial T}{\partial t},$$

$$\left.\frac{\partial T}{\partial x}\right|_{x=0} = 0, \qquad \left.-k\frac{\partial T}{\partial x}\right|_{x=l} = q_1(t),$$

$$\left.\frac{\partial T}{\partial y}\right|_{y=0} = 0, \qquad \left.-k\frac{\partial T}{\partial y}\right|_{y=l} = q_2(t),$$

$$T(x, y, 0) = 0. \tag{18}$$

The second case study demonstrates the ability of the mentioned methods to estimate heat flux in more complicated geometries. The geometry and boundary conditions of the second test case are shown in Figure 2. The entire boundary is considered to be insulated except for the outer wall where a convective heat transfer exists. Figure 2 shows the location and arrangement of the sensors. Assuming constant thermal properties,

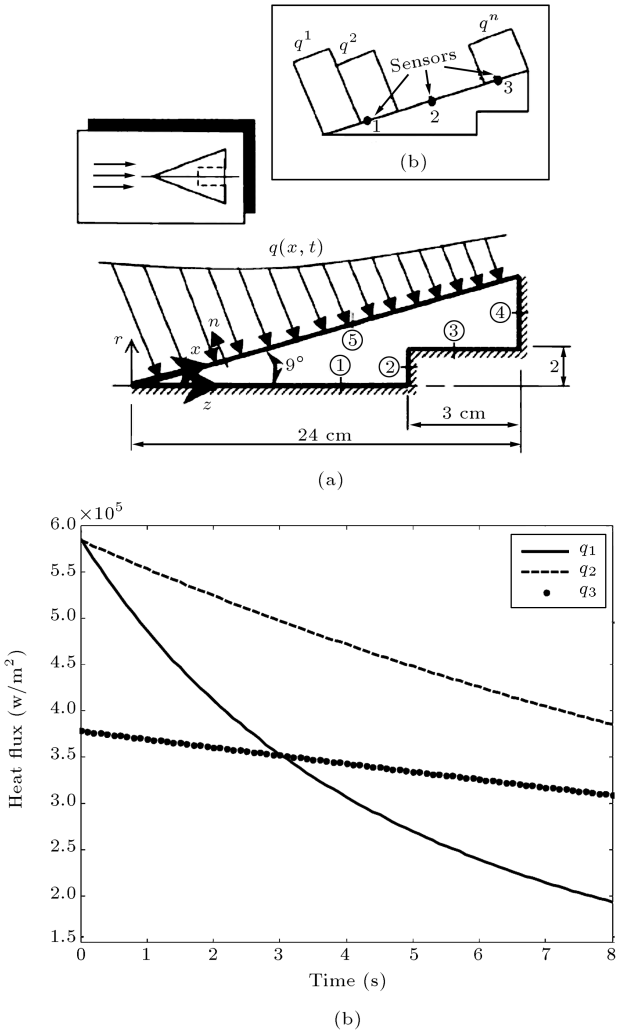

Figure 2. Geometry and boundary conditions of the second case study.

the governing equation is written as:

$$\frac{1}{r}\frac{\partial}{\partial r}\left(r\frac{\partial T}{\partial r}\right) + \frac{\partial^2 T}{\partial z^2} = \frac{1}{\alpha}\frac{\partial T}{\partial t},$$

$$\left.\frac{\partial T}{\partial r}\right|_{(1)} = \left.\frac{\partial T}{\partial z}\right|_{(2)} = \left.\frac{\partial T}{\partial r}\right|_{(3)} = \left.\frac{\partial T}{\partial r}\right|_{(4)} 0,$$

$$\left.-k\frac{\partial T}{\partial n}\right|_{(5)} = q(x,t),$$

$$T(r, z, 0) = 0. \tag{19}$$

CONJUGATE GRADIENT METHOD

The sum of the square of error function shows a difference between measured temperature data and computed temperature:

$$f = \sum_{i=1}^{J}\sum_{m=1}^{M}(T_i(t_m) - Y_i(t_m))^2, \tag{20}$$

in which J is the number of sensors, Y_j is the

temperature measured by the jth sensor and T_j is the corresponding calculated temperature generated by a direct heat conduction model based on a given or assumed vector of $\vec{q}$. In fact, f is our objective function, which is an implicit function of $\vec{q}$ and must be minimized. Methods for solving unconstrained nonlinear optimization are classified into two groups: direct search methods and descent methods. These methods are iterative in nature. The direct search method needs only the objective function value. The descent methods require not only the function value, but also its first and possibly higher order derivatives; therefore, this is also called the gradient based method.

In order to estimate a smoother solution for $\vec{q}$, experimental data are filtered by the mentioned filters before the conjugate gradient algorithm is employed.

Numerical Procedure for the CGM

1. The pulse sensitivity coefficients with respect to each component of $\vec{q}$ are defined as:

$$X_p(x_j, y_j, t_m) = \frac{\partial T(x_j, y_j, t_m)}{\partial q_p^m},$$

$$p = 1, 2, \cdots, P, \qquad j = 1, 2, \cdots, J,$$

$$m = 1, 2, \cdots, n. \tag{21}$$

Governing equations for pulse sensitivity coefficients are obtained by taking the derivative of the heat equation with respect to each q_i^1, which yields:

$$\frac{\partial^2 X}{\partial x^2} + \frac{\partial^2 X}{\partial y^2} = \frac{1}{\alpha}\frac{\partial X}{\partial t},$$

$$\frac{\partial X}{\partial x}\Big|_{x=0} = \frac{\partial X}{\partial y}\Big|_{y=0} = \frac{\partial X}{\partial y}\Big|_{y=l} = 0,$$

$$-k\frac{\partial X}{\partial x}\Big|_{x=l} = \begin{cases} 1 & t_{m-1} \le t \le t_m \\ 0 & \text{others} \end{cases}$$

$$X(x, y, t_{m-1}) = 0. \tag{22}$$

A similar result holds for q_i^2.

2. Smoothed temperatures are calculated as follows:

$$Y_j^s(t), \qquad j = 1, \cdots, J. \tag{23}$$

3. The initial value for $\vec{q}$ is assumed.
4. With respect to an assumed value for $\vec{q}$, the differential equation can be solved and temperatures $[T]$ in the sensors are computed.
5. Stopping (or stoppage) criteria ($\vec{\nabla}_s \le \varepsilon$) is checked here, and if it is not satisfied, the following steps must be followed, otherwise stop the search.
6. The gradient of the objective function at sensor locations is calculated.

$$\vec{\nabla} f = -2[X]^T([Y^s] - [T]). \tag{24}$$

7. Search direction ($\vec{S}$) and the value of search step (γ) are determined here:

$$\vec{S}^k = -\vec{\nabla} f^k + \gamma^k \vec{S}^{k-1},$$

$$\text{if } k = 1 \text{ then } \gamma^1 = 0, \text{ else } \gamma^k = \frac{\left\|\vec{\nabla} f^k\right\|^2}{\left\|\vec{\nabla} f^{k-1}\right\|^2}. \tag{25}$$

8. By assuming $\bar{q}' = \bar{q} + \vec{S}^k$ and the direct solution of the problem, ΔT can be calculated as:

$$\Delta T = T(\bar{q}') - T(\bar{q}). \tag{26}$$

9. The optimal step size is calculated as follows:

$$\beta^k = \frac{\sum_{j=1}^{J}\sum_{m=1}^{M}(T_j(t_m) - Y_j^m(t_m))\Delta T_j(t_m)}{\sum_{j=1}^{k}\sum_{m=1}^{M}\Delta t_j^2(t_m)}. \tag{27}$$

10. A new value for $\vec{q}$ can be obtained:

$$q^{k+1} = q^k + \beta^k S^k. \tag{28}$$

11. Go back to step 3.

THE TIKHONOV REGULARIZATION METHOD

The Tikhonov regularization method is a procedure which modifies the least squares approach by adding terms that are intended to reduce fluctuations in the unknown function, such as the heat flux. These fluctuations are not of a physical origin but are inherent in ill-posed problems unless special treatment is introduced.

The regularization method may have different forms and has been studied by many researchers. The Russians, in particular Tikhonov, Arsenien and Alifanov [1], have pursued various regularization schemes for the IHCP. In the regularization procedure, an augmented sum of squares function, f, is minimized. The whole domain zeroth-order regularization f is defined as:

$$f = \sum_{j=1}^{J}\sum_{i=1}^{n}(Y_j^i - T_j^i)^2 + \alpha\sum_{p=1}^{P}\sum_{i=1}^{n}(q_{p,i})^2. \tag{29}$$

If $\alpha \to 0$, then the exact matching of Y_j and T_j is approached, but the sum of the q_i^2 terms becomes large for small time steps. The effect of a nonzero α is to reduce the magnitude of the q_j values. However, by properly selecting α, instabilities can be reduced because the effect of the regularization term in q_i^2 is to reduce the maximum magnitudes of the estimated values of q_i.

Numerical Procedure for the Tikhonov Regularization Method

As based on what was mentioned previously, sensitivity coefficients are calculated.

1. Smoothed temperatures are calculated as:

$$Y_j^s(t) j = 1, \cdots, J. \tag{30}$$

2. Estimated values for components of heat fluxes are computed as:

$$[q] = [X^T X + \alpha I]^{-1} X^T [Y^s - T_0 I]. \tag{31}$$

In the IHCP, the accuracy and stability are two conflicting objections. For small values of the regularization parameter, the variance error is high, the deterministic bias error is small and vice versa. Thus, an optimal value of the regularization parameter is selected based on the L-shaped graph [1].

SIMULATION OF THE PROBLEM IN ANSYS

The Finite Difference Method (FDM), Finite Volume Method (FVM), Finite Element Method and Boundary Element Method (BEM) are the main numerical methods for solving heat transfer problems. The most attractive feature of the FEM is its ability to handle complicated geometries (and boundaries) with relative ease. The handling of geometries in FEM is theoretically straightforward. In direct calculation, the ANSYS commercial package is used. The finite element mesh contains three-dimensional, four-node thermal elements, PLANE55, with temperature as a single degree of freedom at each node (an axi-symmetric model is used in the second case study). In two cases, it is assumed that the material of the bodies is aluminum. The mesh tool feature and relevant quadric mesh are used in applying the mesh to the geometry. Direct temperatures calculated by the ANSYS as a result of a known imposed heat flux are perturbed by a Gaussian noise with standard deviation of $\sigma = 0.1^\circ$C for the first case study and $\sigma = 1^\circ$C for the second one. The time step used in direct calculations is 0.01 s while this value is 0.1 s for inverse calculations.

RESULTS

The root mean square error is used to compare estimated values with actual values of heat flux. This error is calculated as:

$$\text{erms} = \sqrt{\frac{\sum_{i=1}^{n} (\hat{q}_i - qexact_i)^2}{n}}. \tag{32}$$

The errors in IHCP may be separated into the deterministic bias due to the regularization method and the variance as a result of the sensitivity of the method to the measured errors.

Deterministic bias error can be calculated:

$$D = \sqrt{\frac{\sum_{i=1}^{n} (\hat{q}_{i,\text{without noise}} - qexact_i)^2}{n}}. \tag{33}$$

Variance error is then calculated as:

$$V = \text{erms}^2 - D^2. \tag{34}$$

Note that for better comparison between errors, a second root of variance is used here, while for wavelet calculations and denoising, the wave-menu of the MATLAB toolbox was used. MATLAB uses seven different criteria for thresholding where they can be implemented in either soft or hard thresholding. In our data analysis, we used a conservative thresholding criteria referred to as "penalize high" in MATLAB. These oscillations in hard thresholding were found to be less than those of soft thresholding. We used Db-2 for analyzing wavelet in a multi resolution structure with two levels for decomposition. For a quantitative compression, Tables 1 and 2 show the root mean square error for denoised temperature data by the mentioned

Table 1. Erms ($^\circ$C) for smoothing temperature data by filters in the first case study.

	Wavelet Transform	Moving Average Filter	Mollification Method
Sensor 1	0.0432	0.039	0.04
Sensor 2	0.0522	0.05	0.091

Table 2. Erms ($^\circ$C) for smoothing temperature data by filters in the second case study.

	Moving Average Filter	Wavelet Transform	Mollification Method
Sensor 1	0.44192	1.85021	0.656354
Sensor 2	0.535886	0.761292	0.822335
Sensor 3	0.488204	0.841891	0.740154

filters. It is also obvious from these tables that the moving average filter has a minimum difference smoothed measurement data compared with exact data (without noise). Note that the "exact" word in Figures 3 to 24 means the heat flux for numerical simulation measured temperature data, and the main aim of the mentioned algorithms is its estimation.

Case 1

The results of the conjugate gradient method with and without Discreet Wavelet Transform (DWT) are shown in Figures 3 and 4. The estimated unknown heat fluxes by the CGM with and without a moving average filter (MOA) are shown in Figures 5 and 6. Figures 7 and 8 show the estimated heat fluxes by the conjugate

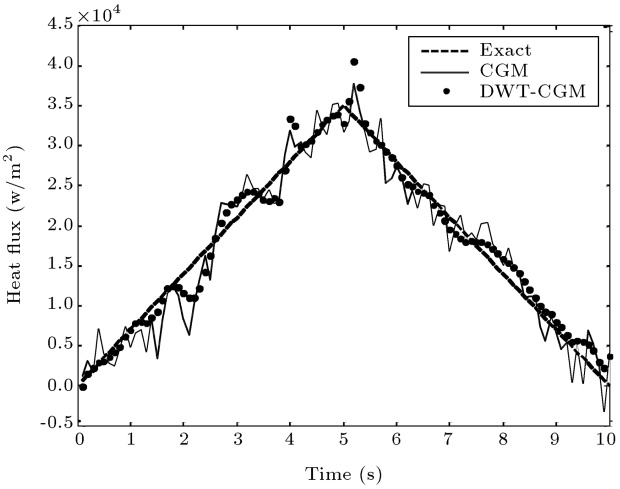

Figure 3. Estimated heat flux value for the first component by CGM by using with and without denoised data by DWT in the first case study.

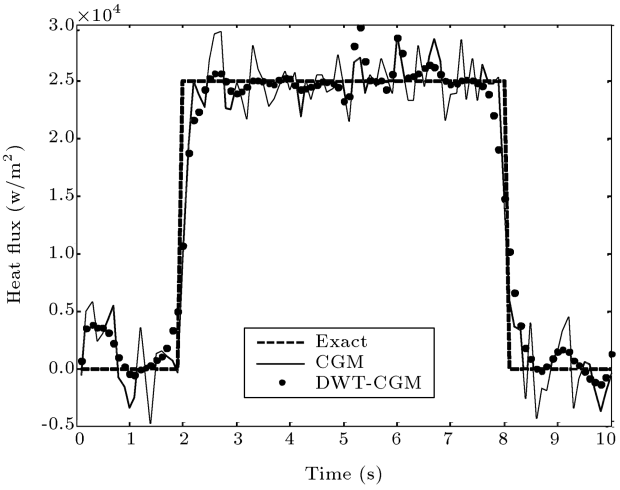

Figure 4. Estimated heat flux value for the second component by CGM by using with and without denoised data by DWT in the first case study.

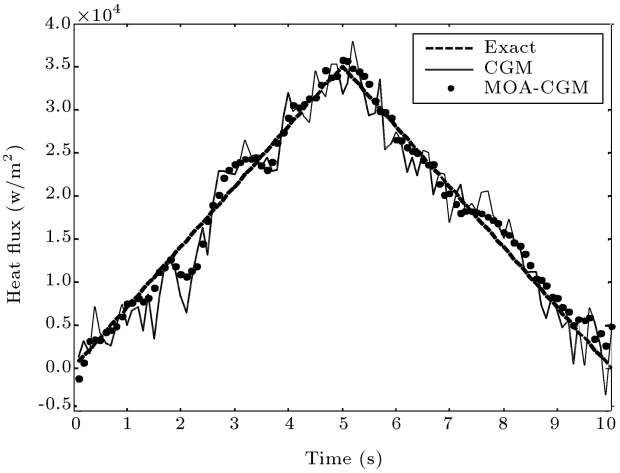

Figure 5. Estimated heat flux value for the first component by CGM by using with and without denoised data by MOA filter in the first case study.

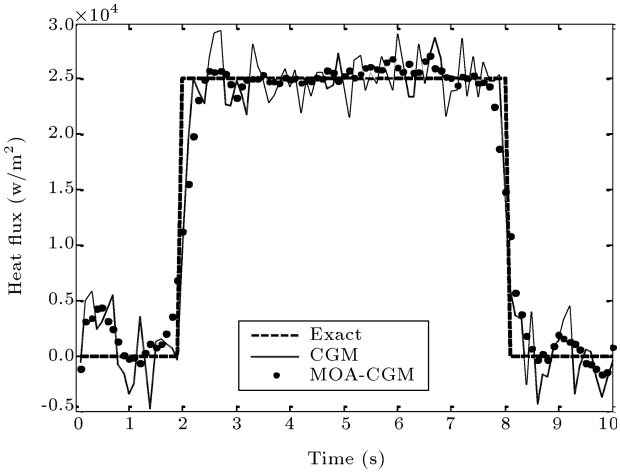

Figure 6. Estimated heat flux value for the second component by CGM by using with and without denoised data by MOA filter in the first case study.

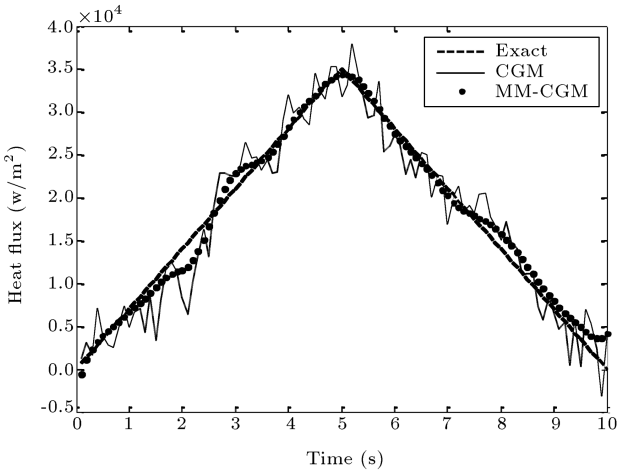

Figure 7. Estimated heat flux value for the first component by CGM by using with and without the mollified data in the first case study.

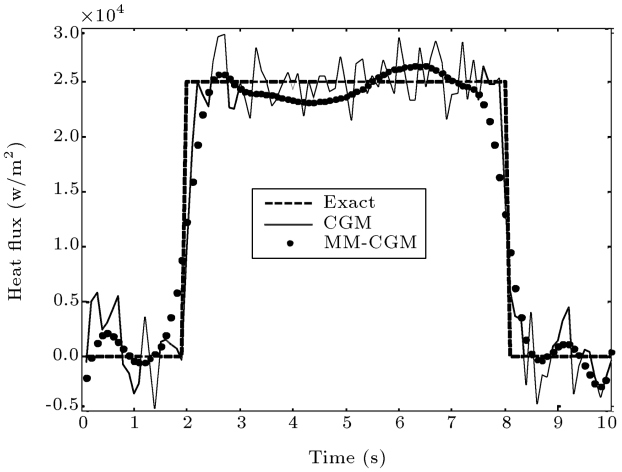

Figure 8. Estimated heat flux value for the second component by CGM by using with and without the mollified data in the first case study.

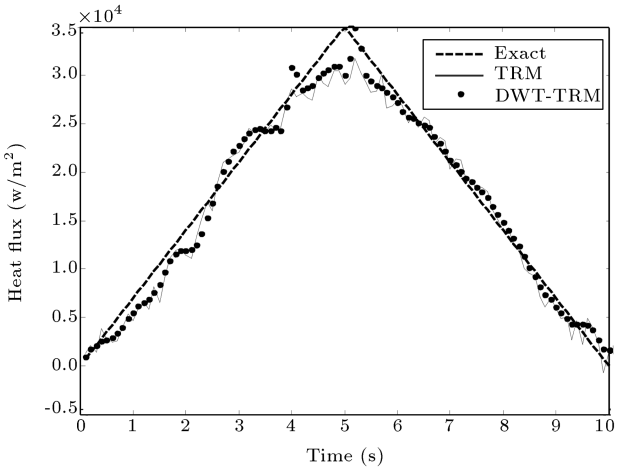

Figure 9. Estimated heat flux value for the first component by TRM by using with and without denoised data by DWT in the first case study.

gradient method with and without mollified data. These figures show smoothed heat flux estimation by denoising the data before the CGM algorithm without a filter. For quantitative compression, the variance, bias and mean square error of the estimated heat flux for noisy data and denoised data are by Wavelet transform. The moving average filter and the mollification method are given in Table 3. It is also obvious in Table 3, which shows this method that smoothing the data has more accuracy and stability than the CGM. The results by the Tikhonov Regularization Method (TRM) with and without Wavelet transform are shown in Figures 9 and 10. Figures 11 and 12 show the results by the Tikhonov Regularization Method (TRM) with and without a moving average filter. The estimated heat flux by TRM, with and without mollified data, is shown in Figures 13 and 14. The regularization parameter value was selected from the corresponding L-curve graph (Figures 15 to 18). These figures show that using a filter to smooth noisy data before the TRM algorithm achieves the smoothed estimation of the unknown heat flux with less error. Table 4 shows an increase in the accuracy and stability of the proposed algorithm, and the regularization parameter (α) value is reduced to a small value.

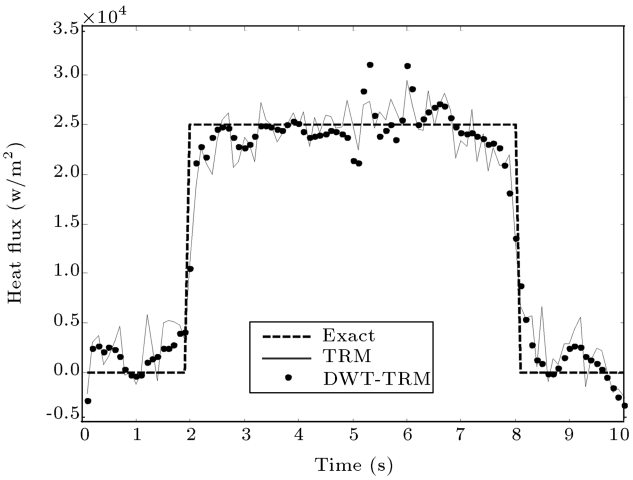

Figure 10. Estimated heat flux value for the second component by TRM by using with and without denoised data by DWT in the first case study.

Case 2

Figure 19 shows the estimated heat fluxes by the conjugate gradient method with and without mollified data. The results by the conjugate gradient method with and without Discreet Wavelet Transform (DWT)

Table 3. Error analysis of estimated heat fluxes by conjugate gradient method with filters in the first case study.

Filter	Component	Erms (w/m^2)	Bias (w/m^2)	Variance (w/m^2)
Wavelet Transform	1	1824.041	414.3014	1776.367
	2	2784.641	1709.218	2198.363
Moving Average Filter	1	1581.724	362.4653	1539.633
	2	2864.831	2351.378	1636.544
Mollification Method	1	1188.638	408.0515	1116.402
	2	3065.416	2935.316	883.57
No Filter	1	2672.485	412.4211	2640.47
	2	3130.227	1709.409	2622.259

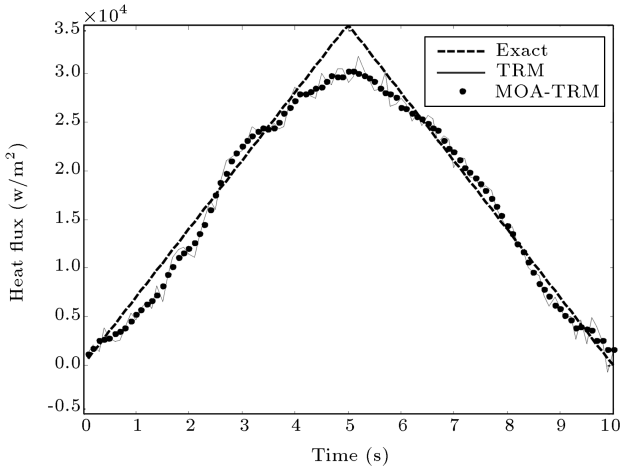

Figure 11. Estimated heat flux value for the first component by TRM by using with and without denoised data by MOA filter in the first case study.

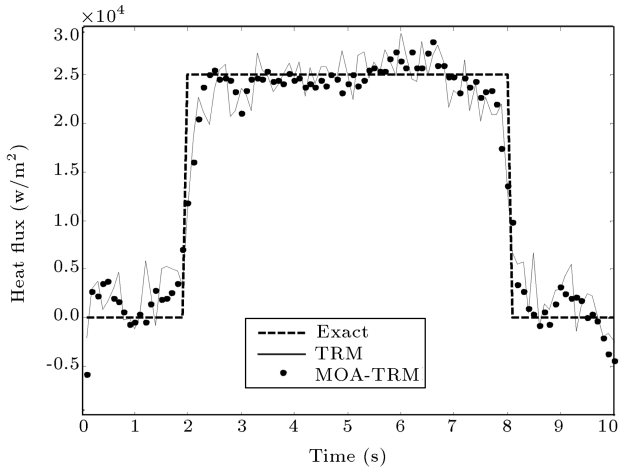

Figure 12. Estimated heat flux value for the second component by TRM by using with and without denoising data by MOA filter in the first case study.

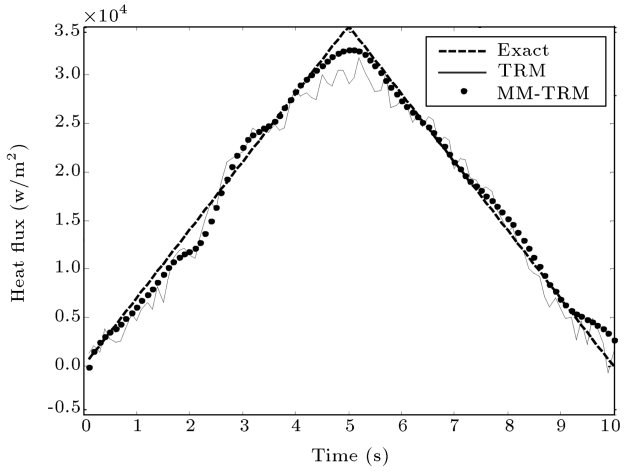

Figure 13. Estimated heat flux value for the first component by TRM by using with and without the mollified data in the first case study.

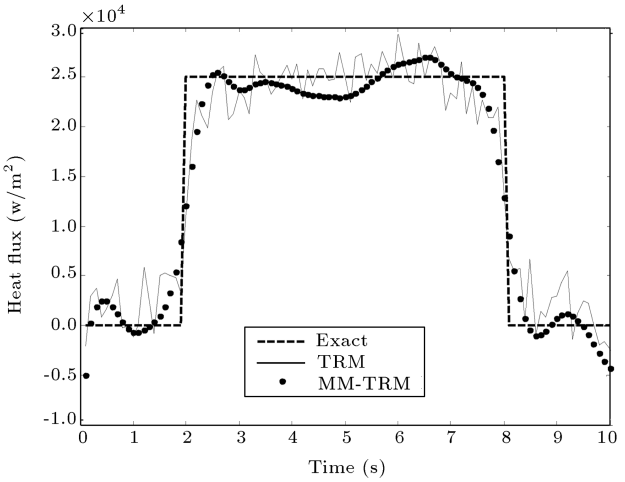

Figure 14. Estimated heat flux value for the second component by TRM by using with and without the mollified data in the first case study.

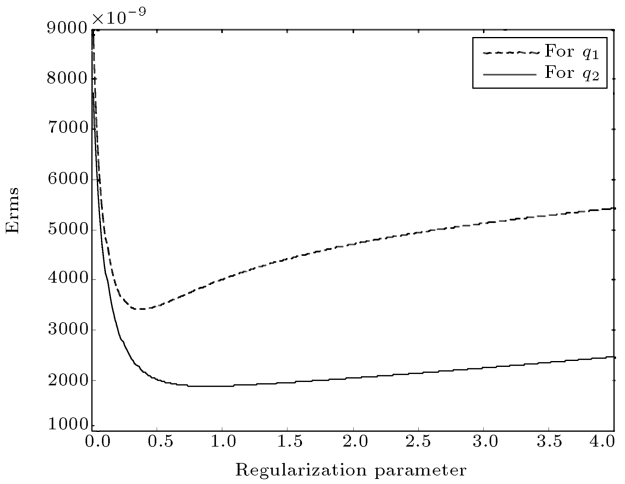

Figure 15. L-curve graph for estimated heat fluxes by TRM in the first case study.

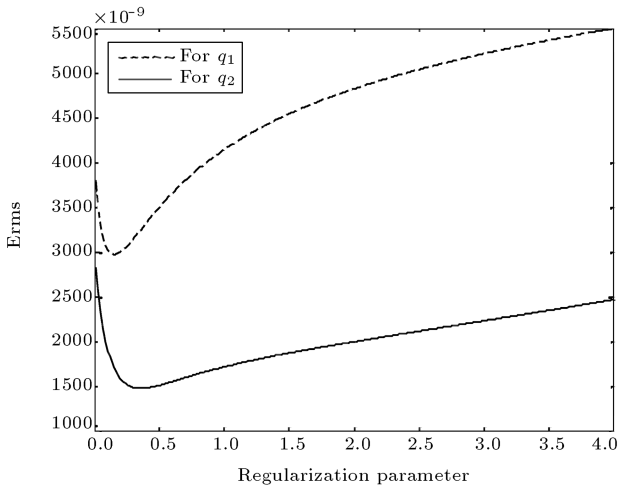

Figure 16. L-curve graph for estimated heat fluxes by TRM with denoised data by DWT in the first case study.

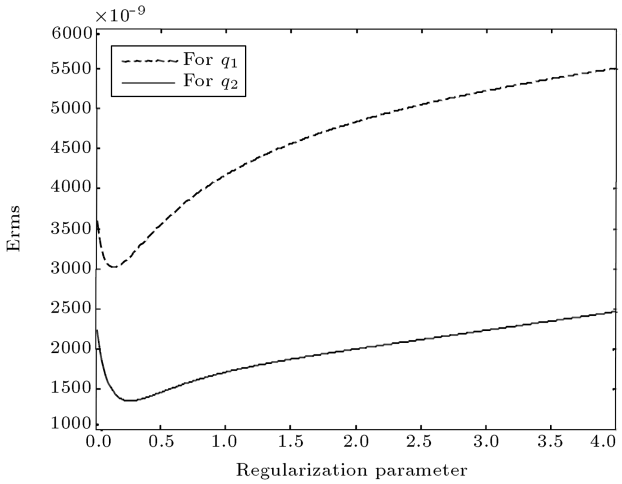

Figure 17. L-curve graph for estimated heat fluxes by TRM with denoised data by MOA in the first case study.

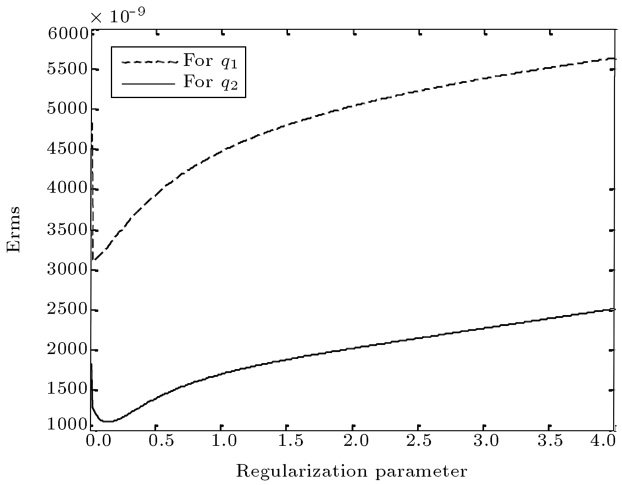

Figure 18. L-curve graph for estimated heat fluxes by TRM with and without the mollified data in the first case study.

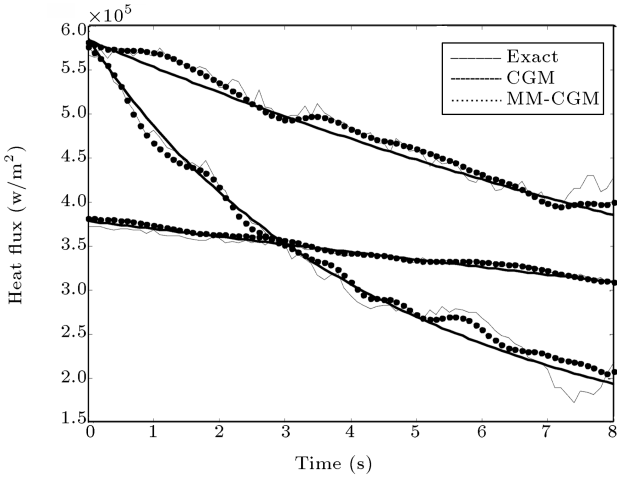

Figure 19. Estimated heat fluxes value by CGM by using with and without the mollified data in the second case study.

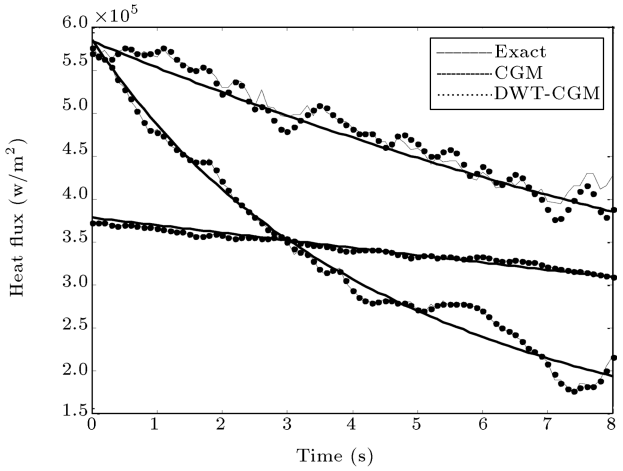

Figure 20. Estimated heat fluxes value by CGM and using denoised data by wavelet transform in the second case study.

are shown in Figure 20. The estimated unknown heat fluxes by the CGM with and without a moving average filter (MOA) are shown in Figure 21. Table 5 shows error analysis for the CGM with and without using denoised data by the mentioned filters. These figures and this table confirm once again the capability of the purposed denoising algorithms. The results by the TRM with and without mollified data are shown in Figure 22. The estimated heat fluxes by the TRM and the DWT-TRM are shown in Figure 23. The results by the TRM and the MOA-TRM are shown in Figure 24. The regularization parameter value was

Table 4. Error analysis of estimated heat fluxes by Tikhonov regularization method with filters in the first case study.

Filter	Component	A	Erms (w/m^2)	Bias (w/m^2)	Variance (w/m^2)
Wavelet Transform	1	1.6E-10	2972.987	1724.568	2421.676
	2	8.8E-10	1663.356	344.6549	1627.257
Moving Average Filter	1	8.8E-10	1663.356	344.6549	1627.257
	2	1.4E-10	3021.255	2372.235	1870.959
Mollification Method	1	1.4E-10	1104.266	381.9836	1036.094
	2	1E-13	3102.099	2914.725	1061.789
No Filter	1	8.8E-10	1876.846	393.6728	1835.095
	2	3.8E-10	3411.004	1724.568	2942.926

Table 5. Error analysis of estimated heat fluxes by conjugate gradient method with filters in the second case study.

Filter	Component	Erms (w/m^2)	Bias (w/m^2)	Variance (w/m^2)
Wavelet Transform	1	14155.91	9035.537	10897.2
	2	13731.97	8243.161	10982.59
	3	3899.461	1109.759	3738.213
Moving Average Filter	1	13084.92	10301.83	8067.683
	2	11082.06	8179.004	7477.7
	3	3746.226	1355.687	3492.323
Mollification Method	1	9947.644	8801.688	4635.29
	2	13831.62	8326.333	11044.73
	3	3549.697	1540.887	3197.814
No Filter	1	14320.38	9408.168	10796.28
	2	14633.26	7887.355	12325.66
	3	4138.234	1019.78	4010.614

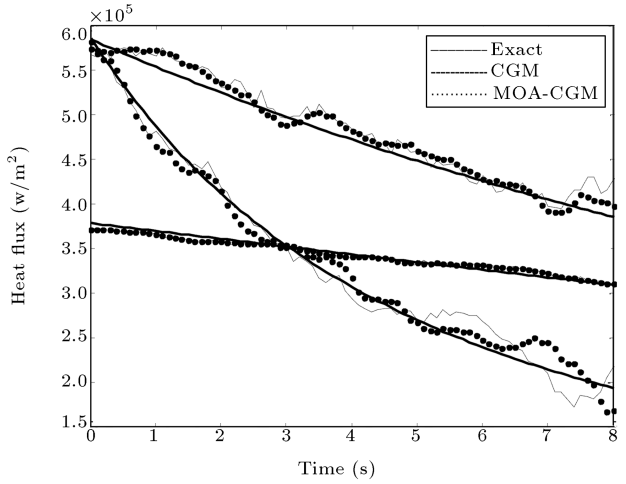

Figure 21. Estimated heat fluxes value by CGM and using denoised data by moving average filter in the second case study.

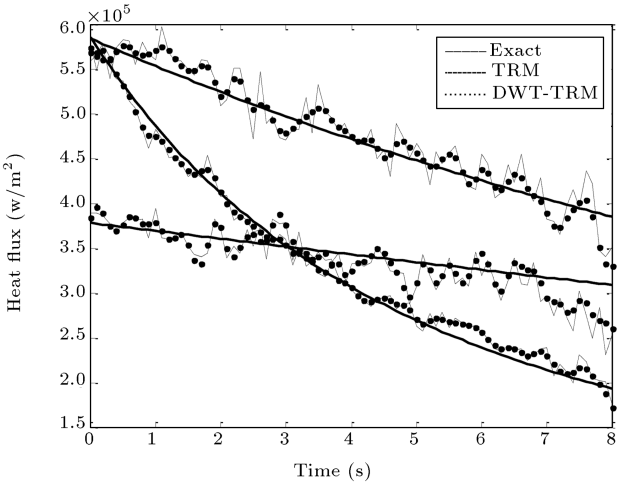

Figure 23. Estimated heat fluxes value by TRM and using denoised data by wavelet transform in the second case study.

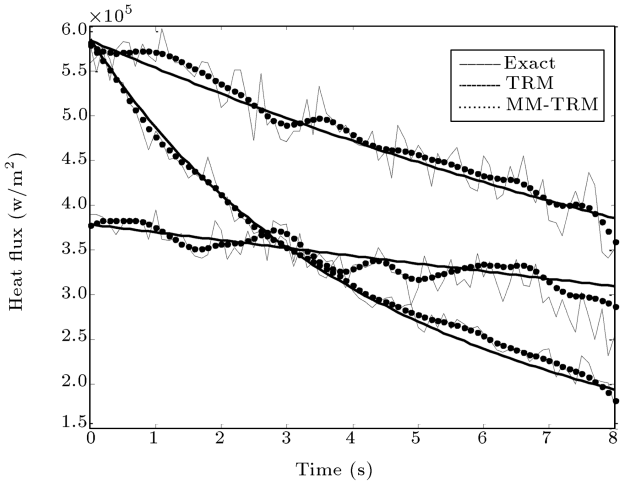

Figure 22. Estimated heat fluxes value by TRM and using denoised data by mollification method in the second case study.

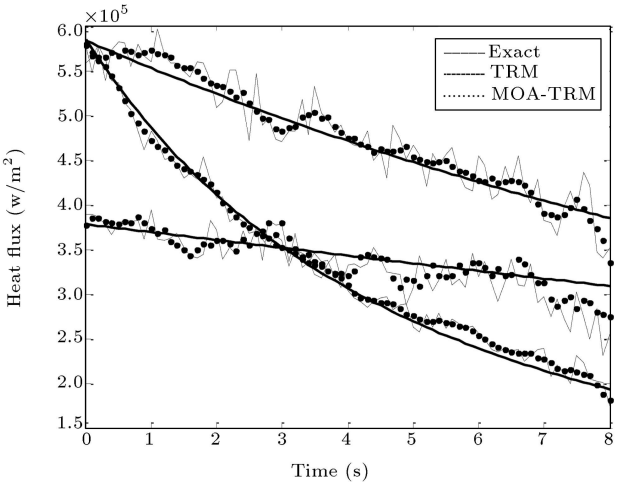

Figure 24. Estimated heat fluxes value by TRM and using denoised data by moving average filter in the second case study.

Table 6. Error analysis of estimated heat fluxes by Tikhonov regularization method with filters in the second case study.

Filter	Component	A	Erms (w/m^2)	Bias (w/m^2)	Variance (w/m^2)
Wavelet Transform	1	1.67E-09	10248.03	8459.725	5784.051
	2	6.4E-10	15735.77	6569.27	14298.92
	3	4.7E-10	18664.69	1269.856	18621.44
Moving Average Filter	1	1.75E-09	9669.554	8418.827	4756.431
	2	5.1E-10	12449.89	6591.445	10561.85
	3	3.1E-10	14726.67	881.1784	14700.29
Mollification Method	1	1.88E-09	7889.638	6253.748	4810.096
	2	3.4E-10	9996.281	6625.23	7485.449
	3	1.4E-10	10989.33	856.987	10955.87
No Filter	1	1.22E-10	15020.89	8253.748	12550.01
	2	7.8E-10	18347.49	6825.23	17030.75
	3	6.8E-10	23178.62	756.987	23166.25

selected from the corresponding L-curve graph, which is not brought here. These figures show the use of a filter to smooth noisy data before the TRM algorithm to achieve a smoothed estimation of the unknown heat flux. Table 6 indicates that applying wavelet transform, moving average filter and the mollification method for noise reduction has an appreciable effect on the TRM algorithm. The results (all figures and tables) show that the mollification method has a better performance in smoothed heat flux estimation than MOA and DWT.

CONCLUSION

By smoothing measured temperature data, the ill-posed inverse heat conduction problem is converted into a well-posed problem that causes an increase in the accuracy and stability of the solution method. Regularization parameters, erms, variance and bias errors in IHCP by using denoised data are reduced. The advantage of using these filters is low-computational loads in the process of solving inverse heat conduction problems. Denoising by wavelet transform and moving average filter has an advantage due to using Toolbox of MATLAB. When the exact temperature data exist, we can use wavelet transform for achieving smoothed noisy data. The code of the mollification method is written easily in programming environments such as MATLAB, ANSYS etc. Using a mollification method to smooth measured data, before the CGM or TRM algorithm, can attain a smoothed estimation of the unknown heat flux with minimum variance error.

REFERENCES

1. Beck, J.V., Blackwell, B. and Clair, S.R., *Inverse Heat Conduction: Ill-Posed Problems*, Wiley, New York (1988).
2. Alifanov, O.M., *Inverse Heat Transfer Problem*, Springer-Verlag, New York (1994).
3. Minkowycz, W.J., Sparrow, E.M., Schneider, G.E. and Pletcher, R.H., Eds., *Handbook of Numerical Heat Transfer*, Wiley, New York (1998).
4. Dowing, K.J., Beck, J.V. and Blackwell, B. "Estimation of direction-dependent thermal properties in a carbon-carbon composite", *Int. J. Heat Mass Tran.*, **39**(5), pp. 3157-3164 (1996).
5. Sun, K. Kim, Bup Sung Jung, Hee June Kim, Wooll lee "Inverse estimation of thermo physical properties for anisotropic composite", *Exp. Therm. Fluid Sci.*, **27**(1), pp. 697-704 (2003).
6. Hsieh, C.K. and Kassab, A.J. "A general method for the solution of inverse heat conduction problem with partially unknown geometries", *Int. J. Heat Mass Tran.*, **29**(1), pp. 47-58 (1986).
7. Lee, H.L., Chang, W.J., Chen, W.L. and Yang, Y.C. "An inverse problem of estimating the heat source in tapered optical fibers for scanning near-field optical microscopy", *Ultra Microscopy*, **107**(1), pp. 656-662 (2007).
8. Tikhonov, A.N. and Arsenin, V.Y., *Solution of Ill-Posed Problems*, Winston and Sons, Washington, DC (1977).
9. Huang, C.-H. and Chen, C.-W. "A boundary-based inverse problem in estimating transient boundary conditions with conjugate gradient method", *International Journal of Numerical Methods in Engineering*, **42**(1), pp. 943-965 (1998).
10. Imber, M. "Two dimensional inverse heat conduction problem further observations", *AIAA*, **J13**, pp. 114-115 (1975).
11. Kakaee, A.H. and Farhanieh, B. "Investigating the effect of different conventional regularization methods on convergence in moving boundary inverse heat conduction problems", *Scientia Iranica*, **11**(1&2), pp. 104-113 (2004).

12. Heydari, M.M. and Farhanieh, B. "An inverse problem method for gas temperature estimation in partially filled rotating cylinders", *Scientia Iranica*, **15**(5), pp. 584-595 (2008).
13. Kowsary, F., Behbahaninia, A. and Pourshaghaghy, A. "Transient heat flux function estimation utilizing the variable metric method", *International Communications in Heat and Mass Transfer (Elsevier)*, **33**(1), pp. 800-810 (2006).
14. Behbahaninia, A. and Kowsary, F. "A dual reciprocity BE-based sequential function specification method for inverse heat conduction problem", *International Journal of Heat and Mass Transfer*, **47**(2), pp. 1247-1255 (2004).
15. Al-Khalidy, N. "On the solution of parabolic and hyperbolic inverse heat conduction problems", *International Journal of Heat and Mass Transfer*, **41**(5), pp. 3731-40 (1998).
16. Ji, C. and Jang, H. "Experimental investigation in inverse heat conduction problem", *Numerical Heat Transfer, Part A.*, **34**(1), pp. 75-91 (1998).
17. Sefidgar, M., Hakkaki-Fard, A. and Kowsary, F. "Application of wavelet in highly ill-posed inverse heat conduction problem", *Heat Transfer Engineering*, **30**(6), pp. 516-527 (2009).
18. Manselli, P. and Miller, K.C. "Calculations of the surface temperature and heat flux on one side of a wall from measurements on the opposite side", *Ann. Mat. Pura Appl.*, **123**, pp. 161-183 (1980).
19. Murio, D.A. "Automatic numerical differentiation by discrete mollification, computers and mathematics", *Applica*, **13**(4), pp. 381-386 (1987).
20. Murio, D.A. "Parameter selection by discrete mollification and the numerical solution of the inverse heat conduction problem", *Journal of Computational and Applied Mathematics*, **22**, pp. 25-34 (1988).
21. Mejia, C.E. and Murio, D.A. "Numerical solution of the generalized IHCP by discrete mollification", *Computer Math. Application*, **32**(2), pp. 33-50 (1996).
22. Donoho, L.D. "Nonlinear wavelet methods for recovery of signals, densities, and spectra from indirect and noisy data", *Different Perspectives on Wavelets, Proceeding of Symposia in Applied Mathematics, Amer. Math. Soc.*, RI, **47**, pp. 173-205 (1993).
23. Donoho, L.D. "Denoising by soft thresholding", *IEEE Trans on Information Theory*, **41**(3), pp. 613-27 (1995).
24. Donoho, L.D. and Johnstone, I.M. "Adapting to unknown smoothness via wavelet shrinkage", *Journal of American Stat. Assoc.*, **90**, pp. 1200-1224 (1995).
25. Mallat, S. "Theories for multiresolution signal decomposition: the wavelet representation", *IEEE Pattern Anal. and Machine Intell.*, **11**(7), pp. 674-93 (1989).

BIOGRAPHIES

Farshad Kowsary is a professor in the field of Heat Transfer at the University of Tehran, Iran. His research interests are in the area of Inverse Heat Transfer with a focus on Inverse Radiation and Conduction. He has a sizable number of papers in the above subjects in reputable heat transfer journals. He is a major reviewer for the Journal of Quantitative Spectroscopy and Radiative Transfer as well as Heat and Mass Transfer.

Somayeh Davoodabadi Farahani obtained her BS in Mechanical Engineering at IUST, Iran in 2007, and her MS in Mechanical Engineering from the University of Tehran in 2009. Her research areas of interest include: The Use of Numerical and Analytical Methods of Solution of the Heat Transfer Problems, Direct Simulation of Thermal Systems, Solution of Inverse Heat Transfer Problems, and Optimization of Thermal Systems.